HHS Public Access

Author manuscript

Int J Radiat Oncol Biol Phys. Author manuscript; available in PMC 2024 May 14.

Published in final edited form as:

Int J Radiat Oncol Biol Phys. 2024 March 15; 118(4): 1110–1122. doi:10.1016/j.ijrobp.2023.10.031.

Antitumor Effect by Either FLASH or Conventional Dose Rate Irradiation Involves Equivalent Immune Responses

Aymeric Almeida, MSc[*], **Céline Godfroid, MSc**[*,†], **Ron J. Leavitt, PhD**[*], **Pierre Montay-Gruel, PhD**[*,‡,§], **Benoit Petit, BSc**[*], **Jackeline Romero, PhD**[*], **Jonathan Ollivier, MSc**[*], **Lydia Meziani, PhD**[*], **Kevin Sprengers, BSc** [‖], **Ryan Paisley, BSc** [‖], **Veljko Grilj, PhD** [‖], **Charles L. Limoli, PhD**[¶], **Pedro Romero, MD, PhD**[†], **Marie-Catherine Vozenin, PhD, HDR**[*]

[*]Laboratory of Radiation Oncology/Radiation Oncology Service/Department of Oncology/CHUV, Lausanne University Hospital and University of Lausanne, Lausanne, Switzerland

[†]Department of Oncology UNIL CHUV, University of Lausanne, Épalinges, Switzerland

[‡]Radiation Oncology Department, Iridium Netwerk, Wilrijk (Antwerp), Belgium

[§]Antwerp Research in Radiation Oncology (AReRO), Centre for Oncological Research (CORE), University of Antwerp, Antwerp, Belgium

[‖]Institute of Radiation Physics, Lausanne University Hospital and Lausanne University, Lausanne, Switzerland

[¶]Department of Radiation Oncology, University of California, Irvine, California

Abstract

Purpose: The capability of ultrahigh dose rate FLASH radiation therapy to generate the FLASH effect has opened the possibility to enhance the therapeutic index of radiation therapy. The contribution of the immune response has frequently been hypothesized to account for a certain fraction of the antitumor efficacy and tumor kill of FLASH but has yet to be rigorously evaluated.

Methods and Materials: To investigate the immune response as a potentially important mechanism of the antitumor effect of FLASH, various murine tumor models were grafted either subcutaneously or orthotopically into immunocompetent mice or in moderately and severely immunocompromised mice. Mice were locally irradiated with single dose (20 Gy) or hypofractionated regimens (3 × 8 or 2 × 6 Gy) using FLASH (≥2000 Gy/s) and conventional (CONV) dose rates (0.1 Gy/s), with/without anti-CTLA-4. Tumor growth was monitored over time and immune profiling performed.

Corresponding author: Marie-Catherine Vozenin; mariecatherine.vozenin@hcuge.ch, marie-catherine.vozenin@chuv.ch.
Aymeric Almeida and Céline Godfroid made equal contributions to this study.
Marie-Catherine Vozenin's current address is Radiotherapy and Radiobiology Sector, Radiation Therapy Service, University Hospital of Geneva, Geneva, Switzerland.

Disclosures: The authors declare no potential conflicts of interest. This work was supported by grants from the National Institutes of Health P01CA244091-01 (M.C.V., C.L.L. to support A.A., V.G.) and Swiss National Science Foundation MAGIC - FNS CRS II5_186369 (M.C.V. to support R.J.L., V.G., K.S., R.P.).

Supplementary material associated with this article can be found, in the online version, at doi:10.1016/j.ijrobp.2023.10.031.

Results: FLASH and CONV 20 Gy were isoeffective in delaying tumor growth in immunocompetent and moderately immunodeficient hosts and increased tumor doubling time to >14 days versus >7 days in control animals. Similar observations were obtained with a hypofractionated scheme, regardless of the microenvironment (subcutaneous flank vs ortho lungs). Interestingly, in profoundly immunocompromised mice, 20 Gy FLASH retained antitumor activity and significantly increased tumor doubling time to >14 days versus >8 days in control animals, suggesting a possible antitumor mechanism independent of the immune response. Analysis of the tumor microenvironment showed similar immune profiles after both irradiation modalities with significant decrease of lymphoid cells by ~40% and a corresponding increase of myeloid cells. In addition, FLASH and CONV did not increase transforming growth factor-β1 levels in tumors compared with unirradiated control animals. Furthermore, when a complete and long-lasting antitumor response was obtained (>140 days), both modalities of irradiation were able to generate a long-term immunologic memory response.

Conclusions: The present results clearly document that the tumor responses across multiple immunocompetent and immune-deficient mouse models are largely dose rate independent and simultaneously contradict a major role of the immune response in the antitumor efficacy of FLASH. Therefore, our study indicates that FLASH is as potent as CONV in modulating antitumor immune response and can be used as an immunomodulatory agent.

Introduction

Ultrahigh dose rate FLASH radiation therapy (RT) has rapidly become one of the most promising therapeutic developments in the field of radiation oncology because of its ability to spare normal tissue while maintaining potent cytotoxic activity on tumors.[1] Understanding the basis of this unexpected differential effect on normal tissues *versus* tumors has been challenging.[2] One popular hypothesis has posited the capability of FLASH to unlock and/or boost the antitumor immune response and thus enhance tumor kill. *In silico* simulation supports this hypothesis[3] and is based on the simple assumption that for a given volume of tissue, the ultrashort time of irradiation would spare a larger fraction of circulating immune cells able to participate in tumor eradication.[4] However, it is possible that FLASH could exhibit immunomodulatory effects comparable to those triggered by conventional (CONV) dose rate irradiation. One could also speculate that the significant reduction in time of irradiation required for FLASH might lead to a tumor cell intrinsic antitumor effect. These different scenarios have not been tested to date.

FLASH aside, understanding the basis of radiation-induced immune activation continues to be a topical area of investigation in the field of radiation oncology. Radiation-induced DNA double strand breaks lead to DNA release in the extracellular milieu during mitotic catastrophe, which induces the activation of the cyclic GMP-AMP synthase (cGAS) −stimulator of interferon genes (STING) pathway and the production of type I interferon involved in immune cell infiltration and T cell responses.[5–7] In addition, radiation-induced immunogenic cell death has been described to generate antigen release and damage-associated molecular patterns such as Adenosine Triphosphate (ATP), High Mobility Group Box 1 (HMGB1), calreticulin membrane-exposure, and extranuclear DNA. These mediators operate on a series of receptors expressed on dendritic cells and trigger their activation.[8,9]

Activated dendritic cells migrate into secondary lymphoid organs where they activate antigen-specific naïve T cells and initiate adaptive T cell responses. Subsequently, activated T cells traffic into blood vessels, infiltrate tumors, and destroy cancer cells.[10] In addition to its local action, RT has also been recognized to elicit a T cell mediated abscopal response on local and distant tumors bearing the same antigens. Despite its many immunostimulatory actions, RT also exerts immunosuppressive effects by direct killing of effector T cells, upregulation of immune checkpoint blockers (eg, Programmed Death-Ligand 1 (PD-L1)) and "don't eat me" CD47 signals, induction of cancer-associated fibroblasts, release of immunosuppressive cytokines (eg, transforming growth factor-β1 (TGF-β)), and recruitment of regulatory T cells and M2 macrophages that collectively alter the efficacy of antitumor immunity.[11,12]

Precisely how to make RT more immunogenic and less immunosuppressive remains unclear, highlighted by the recent unsuccessful radio-immunotherapeutic clinical trials.[13,14] Clearly, more biologic investigations are required to understand the immunomodulatory action of RT and if/how this can be exploited by dose rate modulation. In this context, FLASH could provide a selective advantage compared with CONV because it does not stimulate TGF-β expression, a growth factor known to trigger potent immunosuppressive responses.[15–17]

Considering the foregoing, the present study systematically compared the immunomodulatory imprint triggered by FLASH *versus* CONV on various tumors grown in different mouse models. Results showed equipotency of the 2 modalities in immunocompetent and moderately immunodeficient hosts, irrespective of the organ microenvironment (subcutaneous *vs* orthotopic) and the irradiation regimen (single *vs* hypo-fractionated), with or without immune checkpoint inhibition. These results show that the immunomodulatory action of RT is dose rate independent and refutes hypotheses positing an enhanced immune-mediated antitumor effect of FLASH. Interestingly, FLASH retained antitumor response in severely immunocompromised conditions, suggesting FLASH as a possible strategy for the treatment of cold tumors and/or immunocompromised patients with cancer.

Methods and Materials

Cell culture

Murine SV2, SV2-ovalbumin chicken antigen (OVA), GL261, H454, and human U-87 MG cell lines (Table E1,[18–25]) were cultured in complete medium containing Dulbecco's modified eagle medium (DMEM) + GlutaMAX (4.5g/L D-glucose, pyruvate, 31966–021; Gibco) and supplemented with 10% Fetal Bovin Serum (FBS) for cell culture (F7524; Sigma). Murine mEERL95 cell line was cultured in DMEM/nutrient mixture F 12 medium + GlutaMAX and supplemented with 5% FBS and 1X Human Keratinocyte Growth Supplement (HKGS) (Thermo Fisher Scientific). All cell lines were maintained in an incubator at 37°C, 5% CO_2 and routinely tested to dismiss *Mycoplasma* infection. Before injection, cells were washed with 1X Phosphate Buffer Saline (PBS) (1000324; CHUV), detached with TrypLE Express (without phenol red, 12604–013; Gibco), and counted with Nucleocounter NC-200 (Chemometec). Cells were resuspended in 100% PBS or 60% PBS/

Dulbecco's Phosphate Buffered Saline (DPBS) 1X (-$MgCl_2$, -$CaCl_2$; Gibco) + 40% Matrigel Matrix (356234; Corning) for subcutaneous or orthotopic injection in mice.

Transduction and restimulation assay

SV2 cells were transduced with OVA (Fig. E1) using a previous protocol described in Martinez-Usatorre and Romero.[26] Clonal selection was performed on the SV2-OVA pool population and a single SV2-OVA clone was used for *in vivo* experiments. Mouse OT-1 splenocytes were activated with 1 mg/mL SIINFEKL N4 peptide for 3 days and cultured in complete DMEM. Activated OT-1 were washed and incubated with 10 ng/mL Interleukin-7 (IL-7) to maintain survival (Peprotech #200–07). SV2 cell lines were cultured in complete DMEM. Ten days after activation, OT-1 cells were harvested in medium supplemented with 5 mg/mL soluble aCD28 (Biolegend). SV2 and OT-1 cells were plated at a 1:2 ratio in 96 well-plate and incubated for 6 hours. Surface antibody staining in Fluorescence-activated Cell Sorting (FACS) buffer (2% foetal calf serum (FCS), 2 mmol/L ethylenediaminetetraacetic acid (EDTA) in PBS) was performed in the darkness for 20 min at 4°C. Cells were stained with the following antibodies: CD45.2-BV650 (Biolegend) and CD8-FITC (BioLegend). Aqua fluorescent reactive dye (L34957; Thermo Fisher Scientific) was used for dead cell discrimination. For intracellular cytokine staining, cells were fixed (fixation buffer, 420801; BioLegend) and permeabilized (perm/wash buffer, 421002; BioLegend) before staining with Granzyme B-PE Texas Red (Invitrogen), Interferon (IFN)γ-PerCp-Cy5.5 (cl. XMG1.2; eBioscience), and Tumour Necrosis Factor (TNF)α-APC-Cy7 (cl. MP6-XT22; BioLegend) in perm/wash buffer. Samples were analyzed with an LSRII flow cytometer (BD Biosciences).

Animal experiments

Eight- to nineteen-week-old male and female C57BL/6J mice (Charles River), Swiss nude (NU[Ico]-Foxn1^{nu}) mice (Charles River), and NRG (NOD-Rag1^{null} IL2rg^{null}) mice (Charles River) were used for subcutaneous and orthotopic tumor experiments using SV2 and SV2-OVA lung adenocarcinoma and GL261, H454, and U-87 MG glioblastoma (GBM) cell lines. Female C57BL/6JRJ were purchased from Janvier Labs for experiments using head & neck mEERL95 cell line. All animal experiments were approved by the Swiss ethics committees (Vaud state approval: VD3670 and VD3603) for animal experimentation and performed within institutional guidelines.

Tumor models

For each experimental model, tumors were irradiated with a single dose of 20 Gy or hypofractionated regimens using 2 × 6 Gy and 3 × 8 Gy FLASH or CONV when tumors reached a mean volume of 80 to 100 mm^3. To investigate systemic immunity using abscopal response, mice were treated 3 times with anti-CTLA4 at a dose of 250 μg per animal (clone CD152, BE0131; BioXcell) or control IgG (BE0087; BioXcell) antibodies once every 3 days as shown in Figure E7. Tumor growth was monitored by caliper measurement 3 times a week, and the volume was calculated with the formula of an oblate ellipsoid: $V = (a \times b^2)/2$, where a and b are the minor and major axes of the tumors.

To evaluate the role of the lung microenvironment in the antitumor efficacy of FLASH and CONV, male C57BL/6J mice were injected with SV2-OVA tumor cells in the caudal tail vein in a volume of 200 mL 1X DPBS. Twelve days post-implantation, mice were injected with 1×10^5 OT-1 $CD8^+$ / Vα2 cells in the caudal tail vein. Thirteen and 14 days after SV2-OVA tumor cell injection, mice were irradiated with 2 × 6 Gy with FLASH or CONV dose rate RT delivered to the whole thorax. Mice were scanned twice a week with a micro-computed tomography (MILabs) over the time course of the experiment using a 4-animal bed and total body "accurate" scanning settings. Image reconstruction was done at 50-voxel size. Image analysis was performed using Imalytics Preclinical software (MediLumine). A density threshold based on Hounsfield Units (HU) was determined and used to segment healthy regions of the lungs before 3-dimensional reconstruction. The relative healthy lung volume was calculated using the percentage of initial volume measured at the start of the experiment. Three, 10, or 20 days post-RT, the left lung was collected, embedded in OCT (KMA-0100-00A; CellPath), immediately frozen with dry ice, and cryopreserved at −80°C for hematoxylin/eosin and immunofluorescence staining. The right lungs were collected for immunoprofiling evaluation by flow cytometry.

Mouse irradiation

Irradiations were performed using the eRT6 Oriatron Linear accelerator (PMB-Alcen). This linear accelerator delivers a pulsed electron beam of 5.5 MeV energy[27] at CONV dose rate (0.1 Gy/s) or at ultrahigh dose rate (≥10^7 Gy/s). The beam characteristics were validated to achieve the FLASH effect as previously reported by Montay-Gruel et al.[28] After implantation, subcutaneous tumors of 80 to 100 mm^3 were locally irradiated using a Ø 17-mm^2 circular collimator, with a single dose of 20 Gy or daily fractionated regimens of 2 × 6 Gy or 3 × 8 Gy using CONV or ultrahigh dose rate (FLASH), with the parameters reported in Table E2. For orthotopic tumor experiments, whole thorax irradiation with 2 × 6 Gy CONV or ultrahigh dose rate FLASH was performed using the same collimator. For each experiment, the dose delivery and dosimetry measurements were performed as already described.[29–31]

Clonogenic assay

Murine GL261 GBM cell line was cultured in monolayer with complete medium as described previously and incubated in a hypoxia hood at 4% O_2, 5% CO_2. The next day, cells were harvested, counted, and transferred in 2 mL Eppendorf tubes for irradiation. Irradiation of the tubes was performed in a water tank to ensure a homogeneous distribution of the dose to the target. Irradiations at 2, 4, 6, and 8 Gy using FLASH and CONV parameters are reported in Table E3. Cells were then plated at a concentration of 200 to 2000 cells/well in a 6-well cell culture plate and incubated at 37°C, 5% CO_2 until colonies were visible. Two weeks after irradiation, colonies were fixed, stained with crystal-violet (Sigma), and colonies of >50 cells were counted. Plating efficiency and surviving fractions were determined. The linear quadratic model was used to fit survival curves using Graph-Pad Prism.

Adoptive cell transfer

A spleen from a C57BL/6J OT-1 CD45.1 male mouse was collected and filtered through a 70 mm cell strainer with RPMI medium 1640 + GlutaMAX (61870–010; Gibco), supplemented with 10% FBS. Red blood cells were removed with RBC lysis solution (1045722; Qiagen) for 3 minutes at room temperature. Cells were resuspended in RPMI complete medium and counted with Nucleocounter NC-200 (Chemometec). Single-cell suspensions were stained with LIVE/DEAD Fixable Blue Dead Cell Stain Kit (Thermo Fisher Scientific) for viability. To determine the number of OT1 CD8+/Vα2 cells, cells were surface stained for 20 minutes on ice with CD45.1-FITC (clone A20.1; homemade), CD45.2-PCPCy5.5 (clone 104; Invitrogen), CD8-PE (clone 53.6.7; homemade), and Vα2-APC (clone B20.1; Invitrogen). Cells were resuspended in 1X PBS for caudal vein injection.

Flow cytometry

Right lungs and spleens were mechanically dissociated. Lungs were digested with a mix of enzymes (130.096–730; Miltenyi Biotec) for 30 minutes at 37°C on a thermocycler under 400 rpm agitation. Dissociated lung and spleen tissues were filtered using a 70 mm cell strainer (Corning, Life Science) to generate single-cell suspensions, and spleen cells were resuspended in red blood cell lysis buffer (Qiagen) for 5 minutes at room temperature. Single-cell suspensions were stained with LIVE/DEAD Fixable Blue Dead Cell Stain Kit (ThermoFisher Scientific) for viability. Cells were then incubated with FcR-Block (anti-CD16/32 clone 2.4G2; homemade) for 10 minutes on ice in FACS buffer (2% FBS in PBS). Samples were surface stained for 20 minutes on ice with CD11c-BV421 (clone N418), CD8-BV510 (clone 53–6.7), F4/80-BV605 (clone BM8), NK1.1-BV650 (clone PK136), CD11b-BV711 (clone M1/70), CD4-BV785 (clone RM4–5), CD19-BV785 (clone 6D5), Ly6G-FITC (clone 1A8), CD45.1-BUV661 (clone A20), CD45.2-AF647 (clone 104), GranzymeB-PerCP/Cy5.5 (clone QA16A02), Ki67-AF450 (clone SolA15), CD44-BUV737 (Clone IM7), CD62L-Pe-Cy5 (clone MEL-14), Ly6C-AF700 (clone HK1.4), IA/IE-APC-Cy7(clone M5/114.15.2), and CD3-PE-Cy5.5 (clone 145–2C11) from eBioscience. Cells were fixed with eBioscience Fixation concentrate (2367477; Invitrogen) and diluent (2384234; Invitrogen). Intracellular staining of Foxp3-PeFluor-610 (clone FJK-165; eBioscience) was performed with the Foxp3/Transcription Factor Staining Buffer Set (eBioscience) according to the manufacturer's instructions. Data were acquired using Aurora (Cytek; Flow Cytometry Facility CHUV, UNIL) and the gating strategy is shown in Figure E12.

Histopathology, immunofluorescence, and microscopy

Histologic evaluation of lung parenchyma and tumor area was made using hematoxylin and eosin staining on tissue section and was performed by our histopathology facility (Epalinges, UNIL-CHUV).

For immunofluorescence staining, 8 mm frozen sections were fixed in 2% PFA (15714-S; EMSdiasum). E-cadherin (clone 24E10, 3195; Cell Signaling) staining was used as a structural marker to estimate tumor area. Antimouse CD8a (clone 53–6.7, 14–0081-82; Invitrogen), antimouse CD3 (clone 145–2C11, 16–0031-82; Invitrogen), and antimouse TGF-β1 (polyclonal, NBP1–80289; Novius) were used to quantify CD3+ CD8+ and TGF-

β1 levels. Slides were visualized with an upright Zeiss Axiovision microscope and scanned for image acquisition with a Nanozoomer Slide Scanner. Analyses were performed with QuPath software.

Tumor rechallenge

GBM cells (5×10^6 GL261) were resuspended in a mix of DPBS 1X and Matrigel Matrix and implanted in the left flank of female C57BL/6J mice. When tumors reached 80 to 100 mm^3, mice were irradiated with a single 20 Gy dose of FLASH or CONV, a dose that induced a complete response. At approximately 140 days with complete and stable response, mice were rechallenged with 5×10^6 cells implanted in the opposite (right) flank, and tumor growth was monitored by caliper measurement.

Statistical analysis

Statistical analyses were performed using GraphPad prism (version 9.1). *P* values were estimated from the Mann-Whitney test or the Student *t* test, and the log rank (Mantel-Cox) test was used for survival studies. Kruskal-Wallis with Dunn's multiple comparisons test were performed for doubling time, flow cytometry, and immunofluorescent staining analyses. Results were expressed as the individual value or mean + standard error of the mean and data were deemed significant when $P < .05$.

Results

Effect of the host immune status on tumor response to FLASH *versus* CONV

To investigate if FLASH can enhance the antitumor immune response compared with CONV, we used immunocompetent and immunodeficient mouse strains and a subcutaneous model of lung adenocarcinoma SV2 cells transfected with OVA to enable antigen-specific T cell response. First, SV2-OVA cells were cocultured with activated OT-1 cells, and intracellular productions of Granzyme B, IFNγ, and TNFα were measured to assess the immunogenicity of SV2-OVA adenocarcinoma model. Significant production of Granzyme B, IFNγ, and TNFα was found when OT-1 splenocytes were cocultured with SV2-OVA cells *versus* SV2 cells. Levels were comparable when OT-1 cells were cocultured with the antigenic peptide N4 (SIINFEKL), indicating that OT-1 cells were able to recognize the MHCI−N4 peptide complex presented by our SV2-OVA tumor model (Fig. E2). *In vivo* experiments were performed in immunocompetent mice (C57BL/6J) and in moderately (Swiss Nude) and severely (NRG) immunodeficient mouse strains according to the scheme shown Figure 1A. Two groups of C57BL/6J mice were irradiated with a single dose of 20 Gy FLASH or CONV, a dose known to induce significant tumor growth delay. Tumor doubling time significantly increased to 15.7 days ($P = .002$) and 16.4 days ($P = .0006$) after FLASH and CONV respectively, *versus* 7 days in nonirradiated controls (Figs. 1B, C and E3A). In immunodeficient Swiss nude mice lacking mature T cells, 20 Gy FLASH and CONV induced a similar and significant delay of tumor growth, and significantly increased the tumor doubling time to 14.3 days ($P = .005$) and 16.8 days ($P = .006$), respectively, *versus* 8.1 days in control animals (Figs. 1B, C and E3B). In NRG mice lacking T, B, and NK cells, antitumor efficacy of RT was drastically reduced (Fig. 1B). However, a significant antitumor effect was observed after exposure to FLASH, with a significant increase in the

doubling time of tumors to 14.2 days ($P = .005$) *versus* 8.8 days in control animals (Figs. 1B,C and E3C). To support our findings, similar experiments were performed using several murine and human tumors. In all cases, FLASH and CONV induced equivalent antitumor growth delay, which was not modified by the host immune status (Figs. E4-6). These results show that FLASH and CONV are isoeffective in delaying tumor growth and demonstrate that the tumoricidal activity of RT is more robust in hosts with a functional immune system. Importantly, results obtained in NRG mice indicate that FLASH could remain effective in extreme immunodeficient context whereas CONV would not.

Then, we used 2 clinically relevant hypofractionated schemes, both previously described to increase tumor immunogenicity and antitumor immune response.[32,33] In immunocompetent and immunodeficient mice, 2 × 6 Gy FLASH or CONV induced negligible tumor growth delay (Fig. 2A, B). Interestingly, in immunocompetent animals, 3 × 8 Gy FLASH and CONV significantly increased the doubling time of the tumors to 15.0 days ($P = .002$) and 14.3 days ($P = .01$), respectively, *versus* 6.9 days in control animals (Fig. 2A). Similar results were observed in immunocompromised animals, where 3 × 8 Gy FLASH and CONV significantly increased the doubling time of the tumors to 13.3 days ($P = .01$) and 15.5 days ($P = .001$), respectively, *versus* 8.1 days in control animals (Fig. 2B). In any instance, FLASH and CONV were again isoeffective in delaying tumor growth, an outcome not affected by host immune status and fractionation scheme.

As one of the most potent immunogenic regimens, 3 fractions of 8 Gy has previously been described to generate an abscopal effect in mouse TS/A breast adenocarcinoma and MC-38 colon adenocarcinoma models when combined with an anti-CTLA4 antibody.[32] This experimental approach was used with the SV2-OVA lung adenocarcinoma model to evaluate any abscopal response after FLASH *versus* CONV (Fig. E7A). C57BL/6J mice irradiated with 3 × 8 Gy FLASH or CONV *versus* controls showed similar antitumor responses, confirming our previous observations. Furthermore, the addition of an anti-CTLA4 agent (*vs* IgG control) did not improve the antitumor efficacy of FLASH or CONV at either the primary or distal tumor site (Fig. E7B). These data indicate that the combination of anti-CTLA4 with FLASH or CONV did not potentiate (or otherwise alter) local or systemic immune responses in this model.

Role of tumor microenvironment in modulating antitumor response to FLASH and CONV

Considering the tumor microenvironment (TME) as an important mediator of both tumor progression and treatment efficacy, we then evaluated the possibility of differential TME contribution to the antitumor efficacy of FLASH and CONV using our SV2-OVA tumor model. After orthotopic implantation of SV2-OVA cells in the lung, whole thorax irradiation with 2 daily fractions of 6 Gy was performed according to the schedule shown in Figure 3A. Tumor growth and healthy lung volume were monitored with micro-computer tomography imaging as shown in Figure E8. Tumor growth measurements confirmed that both modalities of irradiation induced equivalent tumor growth delay and improved median survival by 7 days in comparison to untreated tumor-bearing animals (Fig. 3B-D). This result confirms that both modalities induce similar antitumor response and that the lung TME does not affect this response.

FLASH and CONV generate similar remodeling of the lung immune landscape

In the lung, the composition of lymphoid and myeloid compartments was analyzed by flow cytometry at 3, 10, and 20 days post-RT (Figs. 4 and E9). At day 3, both modalities of irradiation induced significant and similar remodeling of both lymphoid and myeloid cell distributions compared with control animals. The lymphoid compartment of control animals was 15.3% CD4+ T cells, 9.7% CD8+ T cells, and 34.5% B cells, whereas those proportions were significantly and similarly reduced to ~8.5%, ~6%, and ~22%, respectively, after irradiation with FLASH and CONV. The myeloid compartment of control animals was 5.8% monocytes and 10.1% granulocytes, populations that were significantly increased to ~14% and ~25%, respectively, after FLASH and CONV.

At 10 *versus* 3 days, most of the immune profile changes were generated by the growth of the tumor itself in untreated control animals, where a decrease in the proportion of lymphoid cells and an increase in the proportion of myeloid cells were found. The lymphoid compartment was composed of 6.4% CD8+ T cells, 25.1% B cells, and 10.9% CD4+ T cells; the myeloid compartment mostly exhibited an increase in the proportion of granulocytes (22.9%). In contrast, FLASH- and CONV-irradiated animals had a similar composition of lymphoid and myeloid cells, and the immune landscape was comparable to what was observed at 3 days post-RT. At 10 days, control animals had similar proportions of proliferative Ki67+ CD4+ T cells (21.3%) and Ki67+ CD8+ T cells (13.5%) compared with 3 days post-RT. Interestingly, these proportions were statistically enhanced to 34.5% and 22% by FLASH whereas the enhancement produced by CONV was slightly lower, respectively to 30% and 18.9%. These data point to a larger contribution of lymphoid cells to the antitumor response induced by irradiation compared with untreated animals (Fig. E9).

At 20 days, control and irradiated animals exhibited a decreased proportion of lymphoid cells and an increased proportion of myeloid cells compared with 3 and 10 days post-RT. The lymphoid compartment in control animals was 9.4% of CD4+ T cells, a proportion that was significantly reduced to ~6.7% after FLASH and CONV. However, although control animals had 11.7% Ki67+ CD4+ T cells, FLASH significantly increased this population to 24.5%, and CONV induced a modest but nonsignificant increase of this population (20.4%; Fig. E9). In the myeloid compartment, control animals had 2.8% monocytes and macrophages, proportions that were significantly increased to ~6.5% after FLASH and CONV. Over the time course of the experiment, the effect of RT on NK cells, dendritic cells, and transferred OT-1+ CD45 + T cells was minimal, indicating a poor contribution of OVA-specific T cells in this model. The flow cytometry results performed on tissue lysates were confirmed by histopathologic examination and immunofluorescence staining. FLASH and CONV groups significantly decreased tumor area to ~29.6% and ~33.5%, respectively, versus 51.5% in control animals (Fig. 5A, C). This result correlated with higher CD3+ CD8+ T cell infiltration (>50%) compared with control animals (21.6%), indicating that FLASH and CONV exerted an immunostimulatory effect on tumors. In the parenchyma, no difference of CD3+ CD8+ T cell infiltration (18%) was found between controls and irradiated animals (Fig. 5B, C). Immunosuppressive signal was also investigated using TGF-β1 staining. We found no modification of intratumoral TGF-β1 expression levels after irradiation and no difference between FLASH and CONV (~0.13%; Fig. E10). These

results provide corroborating histologic evidence that FLASH and CONV exhibit similar efficacy in controlling tumor growth and consistently show that the local immune responses (immunostimulatory and immunosuppressive effects) after FLASH or CONV are similar.

In summary, both radiation modalities were found to be equipotent in delaying the growth of orthotopic SV2-OVA lung tumors and exhibited comparable immune landscapes in the lung. In addition, spleen cell suspensions were analyzed by flow cytometry and no difference was found between FLASH- and CONV-irradiated animals, suggesting similar systemic immune responses (Fig. E11).

Both FLASH and CONV act as *in situ* vaccines

We investigated the capability of FLASH *versus* CONV to induce a complete and sustained antitumor response using a radiation-sensitive GBM cell line, GL261. *In vitro*, the surviving fraction at 2 Gy (SF2) of GL261 cells was ~60% after FLASH or CONV irradiation (Fig. 6A). *In vivo*, 20 Gy FLASH and CONV were able to induce a complete antitumor response in 15 days that was stable without any tumor relapse over 160 days (Fig. 6B). Subsequently, immunologic memory response was evaluated in those animals. Approximately 140 days after complete response, mice were rechallenged with GL261 cells engrafted on the opposite flank. No tumor growth occurred in any of the survivors, whereas GL261 tumors grew in 100% of the untreated naïve animals (Fig. 6C). These results indicate that both irradiation modalities are able to generate equivalent and long-lasting immunologic memory responses.

Discussion

In this study, we performed a systematic and comparative exploration of the immunologic response induced by FLASH and CONV using a panel of syngeneic tumor models. Results show comparable antitumor effects of each radiation modality independent of dose fractionation and the tumor model. Radiation-induced remodeling of the pulmonary TME was also similar between each radiation modality, and upon complete response, both modalities were found to be equally potent operating as *in situ* vaccines. Nevertheless, we were unable to generate radiation-induced abscopal responses after both modalities of irradiation. Although FLASH does not seem to provide any advantage over CONV at the immunologic level, it does induce an antitumor response in severely immunocompromised hosts.

Understanding the immunomodulatory potential of RT and the mechanistic basis of the FLASH effect are topical areas of interest in radiation oncology. Of the many mechanisms proposed to account for the FLASH effect, those that posit sparing of circulating immune cells are not supported by the findings presented in this study. A computational study was the first to suggest a possible sparing effect of circulating immune cells by FLASH,[3] a hypothesis further developed by Zhang et al,[4] ideas at the time that were not supported by solid experimental evidence. Although one report showed a modest but significant increase of CD8+ T cells after FLASH (7.5%) *versus* CONV (6%) in Lewis lung carcinoma,[34] the preponderance of other studies have shown similar antitumor immune contributions between FLASH and CONV. The antitumor effect of FLASH and CONV was shown to be similar in human and murine lung,[15,35] head and neck,[17] sarcoma,[16] pancreatic,[34] GBM,[36] and

ovarian tumors[37] grown in immunocompetent and immunodeficient mouse models and was recently shown in immunocompetent rats engrafted with glioblastoma.[38,39] Consistently, using doses delivered in 1 or 2 pulses with electron FLASH or >1000 pulses with CONV, we found similar antitumor responses in immunocompetent and partially immunodeficient mouse strains. Remodeling of the immune landscape was also found to be similar, without any significant difference in the subpopulations found after either irradiation modality. These results are consistent with previous findings showing similar distributions of macrophages, B cells, monocytes, and activated and naïve T cells in the normal lung parenchyma after 17 Gy electron FLASH and CONV.[35] More recently, in an intraperitoneal ID8 tumor model, 14 Gy electron FLASH and CONV were found to decrease the proportion of CD45+ immune cells, T cells, and CD4+ T cells at 96 hours post-RT, again with no significant difference between the 2 irradiation modalities.[37] Importantly, in this study, the addition of anti-PD-1 treatment increased the proportion of CD8+ T cells after both FLASH and CONV compared with controls, with little differential effect on immune distribution.[37] The dose rate independence of the immune response is also supported by recent work showing similar immune profiles in an orthotopic rat glioma model after exposure to proton FLASH and CONV.[39] Although our results show that intratumoral immunostimulatory signals triggered by RT are dose rate independent, the repression of immunosuppressive signals could compensate and explain the antitumor efficacy of FLASH. In normal tissues (lung, skin, and gut), previous studies indeed showed that TGF-β1 expression was reduced after FLASH exposure.[15,17] However, in our study, TGF-β1 expression was not modified in SV2 OVA lung adenocarcinoma exposed to FLASH or CONV. Although our study is limited to TGF-β1 expression in one tumor model, it highlights the contrasting responses to dose rate observed in normal tissues *versus* tumors and supports the idea that FLASH and CONV induce similar immune responses in lung tumors. Finally, we show here that immune remodeling is not modified by fractionation regimen, and recently Iturri et al[39] showed a similar trend with proton-FLASH. This suggests that the temporal structures of pulsed electron beams and semi-continuous proton beams do not differentially affect the immune response but rather elicit an equal effect on local lymphoid and myeloid cell distributions in tissues.

To further characterize the antitumor immune response generated upon FLASH, the activation of systemic immunity was evaluated using abscopal and immunologic memory responses as surrogate readouts. Although radiation-induced abscopal responses have been described, they have proven difficult to reproduce routinely. The work by Vanpouille-Box et al[40] showed that a 3 × 8 Gy regimen was able to increase immune-mediated local and abscopal responses when combined with an anti-CTLA4 antibody in mouse TS/A breast and MC-38 colon cancer models.[32] Mechanistically, CTLA4 expression on T cells blunts T cell activation through interaction with CD80 expressed on dendritic cells during antigen presentation and impairs tumor cell killing by T cells. Using a similar strategy in our mouse lung model, local and systemic immune benefits were not found by combining FLASH or CONV with anti-CTLA4 blockade. This result is, however, consistent with findings from a recent study using the MC-38 colorectal tumor model, where equal local and abscopal responses were reported after 5 × 5 Gy x-ray FLASH and CONV were combined with anti-PD-L1 treatment.[41]

Another important aspect of the immune response is the formation of immunologic memory, known to provide long-term protective immunity against infections and other diseases including cancer. To investigate this question, we used a highly aggressive, moderately immunogenic, but radiosensitive GBM GL261 model, which provides a tractable tool to investigate complete tumor responses, recurrence, and immunologic memory responses. In the present work, FLASH and CONV were found equipotent at generating a complete response when GL261 tumors were grown subcutaneously. Upon rechallenge, tumor rejection indicates that both irradiation modalities promoted a persistent immunologic memory response. These results are consistent with data showing that 2 × 8 Gy electron FLASH and CONV induced similar long-term tumor control of NS1 glioblastoma orthotopically grafted in immunocompetent rats, along with memory response upon rechallenge.[38] Collectively, these data provide convincing evidence that both FLASH and CONV generate similar local and systemic tumor immune responses.

The focus of our study was to elucidate the role (if any) of dose rate modulation on the immune response of select mouse tumor models. To that end, we have established that the immune hypothesis fails to provide a satisfactory explanation for the antitumor efficacy of FLASH. Current findings also corroborate with recent work showing that FLASH is efficient against radioresistant hypoxic tumors (Leavitt et al., 2023, in revision). Another innovative aspect of the present work is related to the antitumor response of FLASH in profoundly immunodeficient animals, pointing to the potential utility of this approach in controlling immunologically cold tumors and/or treating immune-compromised patients.[42] In support of the latter, patients with HIV treated for cervical cancer with external beam RT,[43] 3-dimensional conformal RT,[44] and cobalt 60 RT[45] are at higher risks of skin, gastrointestinal, and genitourinary toxicities, adverse outcomes that could be minimized with FLASH. Similar benefits could also be applied in patients with anal cancer, where acute toxicity often translates into significant reductions in therapeutic management and poorer survival.[46–48] In these and other sensitive patient populations, FLASH may provide dual benefits of ameliorating adverse radiation-induced normal tissue toxicities while retaining efficient tumor control.

Conclusion

In summary, our study shows that local and systemic immune responses are dose rate independent. In addition, our study opens a potentially new area of investigation as FLASH retains antitumor response in a severely immunodeficient context. Thus, FLASH may soon provide another useful tool for the treatment of more challenging immunocompromised patients with cancer.

Supplementary Material

Refer to Web version on PubMed Central for supplementary material.

Acknowledgments—

The authors thank Prs J. Bourhis and F. Bochud for their support, and Pr G. Tolstonog for the OVA construct. We also thank the Lausanne core facilities including the animal facility, cellular imaging facility, in vivo imaging facility, and mouse pathology facility at Epalinges.

Statment regarding data sharing:

Research data are stored in an institutional repository and will be shared uponrequest to the corresponding author.

References

1. Vozenin M-C, Hendry JH, Limoli CL. Biological benefits of ultra-high dose rate FLASH radiotherapy: Sleeping beauty awoken. Clin Oncol (R Coll Radiol) 2019;31:407–415. [PubMed: 31010708]
2. Limoli CL, Vozenin M-C. Reinventing radiobiology in the light of FLASH radiotherapy. Ann Rev Cancer Biol 2023;7:1–21.
3. Jin J-Y, Gu A, Wang W, et al. Ultra-high dose rate effect on circulating immune cells: A potential mechanism for FLASH effect? Radiother Oncol 2020;149:55–62. [PubMed: 32387486]
4. Zhang Y, Ding Z, Perentesis JP, et al. Can rational combination of ultra-high dose rate FLASH radiotherapy with immunotherapy provide a novel approach to cancer treatment? Clin Oncol 2021;33:713–722.
5. Eriksson D, Stigbrand T. Radiation-induced cell death mechanisms. Tumour Biol 2010;31:363–372. [PubMed: 20490962]
6. Gekara NO. DNA damage-induced immune response: Micronuclei provide key platform. J Cell Biol 2017;216:2999–3001. [PubMed: 28860276]
7. Harding SM, Benci JL, Irianto J, et al. Mitotic progression following DNA damage enables pattern recognition within micronuclei. Nature 2017;548:466–470. [PubMed: 28759889]
8. Ashrafizadeh M, Farhood B, Eleojo Musa A, et al. Damage-associated molecular patterns in tumor radiotherapy. Int Immunopharmacol 2020;86 106761.
9. Lumniczky K, Sáfrány G. The impact of radiation therapy on the antitumor immunity: Local effects and systemic consequences. Cancer Lett 2015;356:114–125. [PubMed: 23994343]
10. Chen DS, Mellman I. Oncology meets immunology: The cancer-immunity cycle. Immunity 2013;39:1–10. [PubMed: 23890059]
11. Ngwa W. Using immunotherapy to boost the abscopal effect. Nat Rev Cancer 2018;18:313–322. [PubMed: 29449659]
12. Arina A, Beckett M, Fernandez C, et al. Tumor-reprogrammed resident T cells resist radiation to control tumors. Nat Commun 2019;10:3959. [PubMed: 31477729]
13. Theelen WSME, Peulen HMU, Lalezari F, et al. Effect of pembrolizumab after stereotactic body radiotherapy versus pembrolizumab alone on tumor response in patients with advanced non-small cell lung cancer: Results of the PEMBRO-RT phase 2 randomized clinical trial. JAMA Oncol 2019;5:1276–1282. [PubMed: 31294749]
14. Schoenfeld JD, Giobbie-Hurder A, Ranasinghe S, et al. Durvalumab plus tremelimumab alone or in combination with low-dose or hypofractionated radiotherapy in metastatic non-small-cell lung cancer refractory to previous PD(L)-1 therapy: An open-label, multicentre, randomised, phase 2 trial. Lancet Oncol 2022;23:279–291. [PubMed: 35033226]
15. Favaudon V, Caplier L, Monceau V, et al. Ultrahigh dose-rate FLASH irradiation increases the differential response between normal and tumor tissue in mice. Sci Transl Med 2014;6 245ra93–245ra93.
16. Velalopoulou A, Karagounis IV, Cramer GM, et al. FLASH proton radiotherapy spares normal epithelial and mesenchymal tissues while preserving sarcoma response. Cancer Res 2021;81:4808–4821. [PubMed: 34321243]

17. Cunningham S, McCauley S, Vairamani K, et al. FLASH proton pencil beam scanning irradiation minimizes radiation-induced leg contracture and skin toxicity in mice. Cancers (Basel) 2021;13:1012. [PubMed: 33804336]
18. Groeneveld S, Faget J, Zangger N, Meylan E. Snail mediates repression of the Dlk1-Dio3 locus in lung tumor-infiltrating immune cells. Oncotarget 2018;9:32331–32345. [PubMed: 30190790]
19. Mermod M, Hiou-Feige A, Bovay E, et al. Mouse model of postsurgical primary tumor recurrence and regional lymph node metastasis progression in HPV-related head and neck cancer. Int J Cancer 2018;142:2518–2528. [PubMed: 29313973]
20. Seligman AM, Shear MJ, Alexander L. Studies in carcinogenesis: VIII. Experimental production of brain tumors in mice with methylcholanthrene1. Am J Cancer Res 1939;364–395.
21. Shchors K, Massaras A, Hanahan D. Dual targeting of the autophagic regulatory circuitry in gliomas with repurposed drugs elicits cell-lethal autophagy and therapeutic benefit. Cancer Cell 2015;28:456–471. [PubMed: 26412325]
22. Pontén J, Macintyre EH. Long term culture of normal and neoplastic human glia. Acta Pathol Microbiol Scand 1968;74:465–486. [PubMed: 4313504]
23. Allen M, Bjerke M, Edlund H, Nelander S, Westermark B. Origin of the U87MG glioma cell line: Good news and bad news. Sci Transl Med 2016;8:354re3.
24. Brattain MG, Levine AE, Chakrabarty S, Yeoman LC, Willson JK, Long B. Heterogeneity of human colon carcinoma. Cancer Metastasis Rev 1984;3:177–191. [PubMed: 6437669]
25. Boyd D, Florent G, Kim P, et al. Determination of the levels of urokinase and its receptor in human colon carcinoma cell lines. Cancer Res 1988;48:3112–3116. [PubMed: 2835152]
26. Martinez-Usatorre A, Romero P. Generation of affinity ranged antigen-expressing tumor cell lines. In: Galluzzi L, Rudqvist N-P, eds. Methods in Enzymology. Vol 632. Tumor Immunology and Immunotherapy − Cellular Methods Part B. Academic Press; 2020:503–519.
27. Jorge PG, Jaccard M, Petersson K, et al. Dosimetric and preparation procedures for irradiating biological models with pulsed electron beam at ultra-high dose-rate. Radiother Oncol 2019;139:34–39. [PubMed: 31174897]
28. Montay-Gruel P, Petersson K, Jaccard M, et al. Irradiation in a flash: Unique sparing of memory in mice after whole brain irradiation with dose rates above 100Gy/s. Radiother Oncol 2017;124:365–369. [PubMed: 28545957]
29. Jaccard M, Petersson K, Buchillier T, et al. High dose-per-pulse electron beam dosimetry: Usability and dose-rate independence of EBT3 Gafchromic films. Med Phys 2017;44:725–735. [PubMed: 28019660]
30. Jaccard M, Durán MT, Petersson K, et al. High dose-per-pulse electron beam dosimetry: Commissioning of the Oriatron eRT6 prototype linear accelerator for preclinical use. Med Phys 2018;45:863–874. [PubMed: 29206287]
31. Petersson K, Jaccard M, Germond J-F, et al. High dose-per-pulse electron beam dosimetry - A model to correct for the ion recombination in the Advanced Markus ionization chamber. Med Phys 2017;44:1157–1167. [PubMed: 28094853]
32. Dewan MZ, Galloway AE, Kawashima N, et al. Fractionated but not single-dose radiotherapy induces an immune-mediated abscopal effect when combined with anti−CTLA-4 antibody. Clin Cancer Res 2009;15:5379–5388. [PubMed: 19706802]
33. Labiano S, Roh V, Godfroid C, et al. CD40 Agonist targeted to fibroblast activation protein α synergizes with radiotherapy in murine HPV-positive head and neck tumors. Clin Cancer Res 2021;27:4054–4065. [PubMed: 33903200]
34. Kim Y-E, Gwak S-H, Hong B-J, et al. Effects of ultra-high doserate FLASH irradiation on the tumor microenvironment in Lewis lung carcinoma: Role of myosin light chain. Int J Radiat Oncol Biol Phys 2021;109:1440–1453. [PubMed: 33186615]
35. Fouillade C, Curras-Alonso S, Giuranno L, et al. FLASH irradiation spares lung progenitor cells and limits the incidence of radio-induced senescence. Clin Cancer Res 2020;26:1497–1506. [PubMed: 31796518]
36. Montay-Gruel P, Acharya MM, Jorge PG, et al. Hypofractionated FLASH-RT as an effective treatment against glioblastoma that reduces neurocognitive side effects in mice. Clin Cancer Res 2021;27:775–784. [PubMed: 33060122]

37. Eggold JT, Chow S, Melemenidis S, et al. Abdominopelvic FLASH irradiation improves PD-1 immune checkpoint inhibition in preclinical models of ovarian cancer. Mol Cancer Ther 2022;21:371–381. [PubMed: 34866044]
38. Liljedahl E, Konradsson E, Gustafsson E, et al. Long-term antitumor effects following both conventional radiotherapy and FLASH in fully immunocompetent animals with glioblastoma. Sci Rep 2022;12:12285. [PubMed: 35853933]
39. Iturri L, Bertho A, Lamirault C, et al. Proton FLASH radiation therapy and immune infiltration: Evaluation in an orthotopic glioma rat model. Int J Radiat Oncol Biol Phys 2022;116:655–665. [PubMed: 36563907]
40. Vanpouille-Box C, Alard A, Aryankalayil MJ, et al. DNA exonuclease Trex1 regulates radiotherapy-induced tumour immunogenicity. Nat Commun 2017;8:15618. [PubMed: 28598415]
41. Shi X, Yang Y, Zhang W, et al. FLASH X-ray spares intestinal crypts from pyroptosis initiated by cGAS-STING activation upon radioimmunotherapy. Proc Natl Acad Sci USA 2022;119:e2208506119.
42. Alongi F, Giaj-Levra N, Sciascia S, et al. Radiotherapy in patients with HIV: Current issues and review of the literature. Lancet Oncol 2017;18: e379–e393. [PubMed: 28677574]
43. Dryden-Peterson S, Bvochora-Nsingo M, Suneja G, et al. HIV infection and survival among women with cervical cancer. J Clin Oncol 2016;34:3749–3757. [PubMed: 27573661]
44. Simonds HM, Neugut AI, Jacobson JS. HIV status and acute hematologic toxicity among patients with cervix cancer undergoing radical chemoradiation. Int J Gynecol Cancer 2015;25:884–890. [PubMed: 25853380]
45. Gichangi P, Bwayo J, Estambale B, et al. HIV impact on acute morbidity and pelvic tumor control following radiotherapy for cervical cancer. Gynecol Oncol 2006;100:405–411. [PubMed: 16274737]
46. Munoz-Bongrand N, Poghosyan T, Zohar S, et al. Anal carcinoma in HIV-infected patients in the era of antiretroviral therapy: A comparative study. Dis Colon Rectum 2011;54:729–735. [PubMed: 21552058]
47. Oehler-Jänne C, Huguet F, Provencher S, et al. HIV-specific differences in outcome of squamous cell carcinoma of the anal canal: A multicentric cohort study of HIV-positive patients receiving highly active antiretroviral therapy. J Clin Oncol 2008;26:2550–2557. [PubMed: 18427149]
48. Xu MJ, Liewen A, Valle L, et al. Organ-specific toxicities due to radiation therapy in cancer patients with or without HIV infection: A systematic review of the literature. Front Oncol 2018;8:276. [PubMed: 30105217]

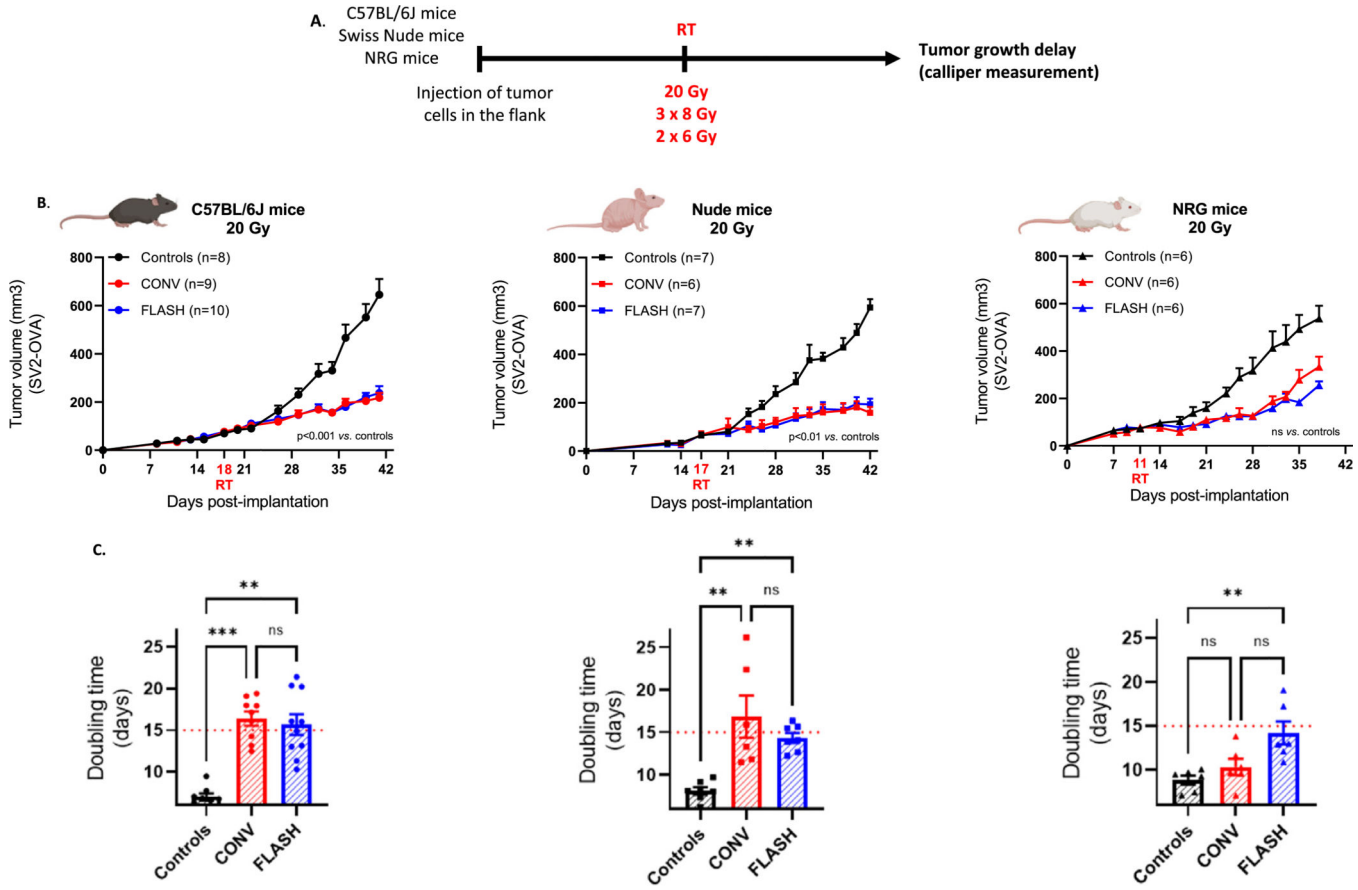

Fig. 1.

FLASH retains antitumor response in severe immunocompromised host. SV2-OVA lung adenocarcinoma were irradiated at 20 Gy with FLASH or CONV after subcutaneous engraftment into immunocompetent C57BL/6J male mice, moderate immunodeficient Swiss nude male mice, and severely immunodeficient NRG (NOD-Rag1null IL2rgnull) male mice, and tumor growth delay was followed by caliper measurement 3 times per week (A,B). Doubling time of tumors was determined using the model of exponential (Malthusian) growth from relative tumor growth curves on GraphPad Prism (C). Results are given in mean + standard error of the means. Statistical analysis of growth curves was performed using Mann-Whitney test. Kruskal-Wallis with Dunn's multiple comparisons test was assessed for doubling time analysis. $*P < .05$, $**P < .01$, $***P < .001$, $****P < .0001$.

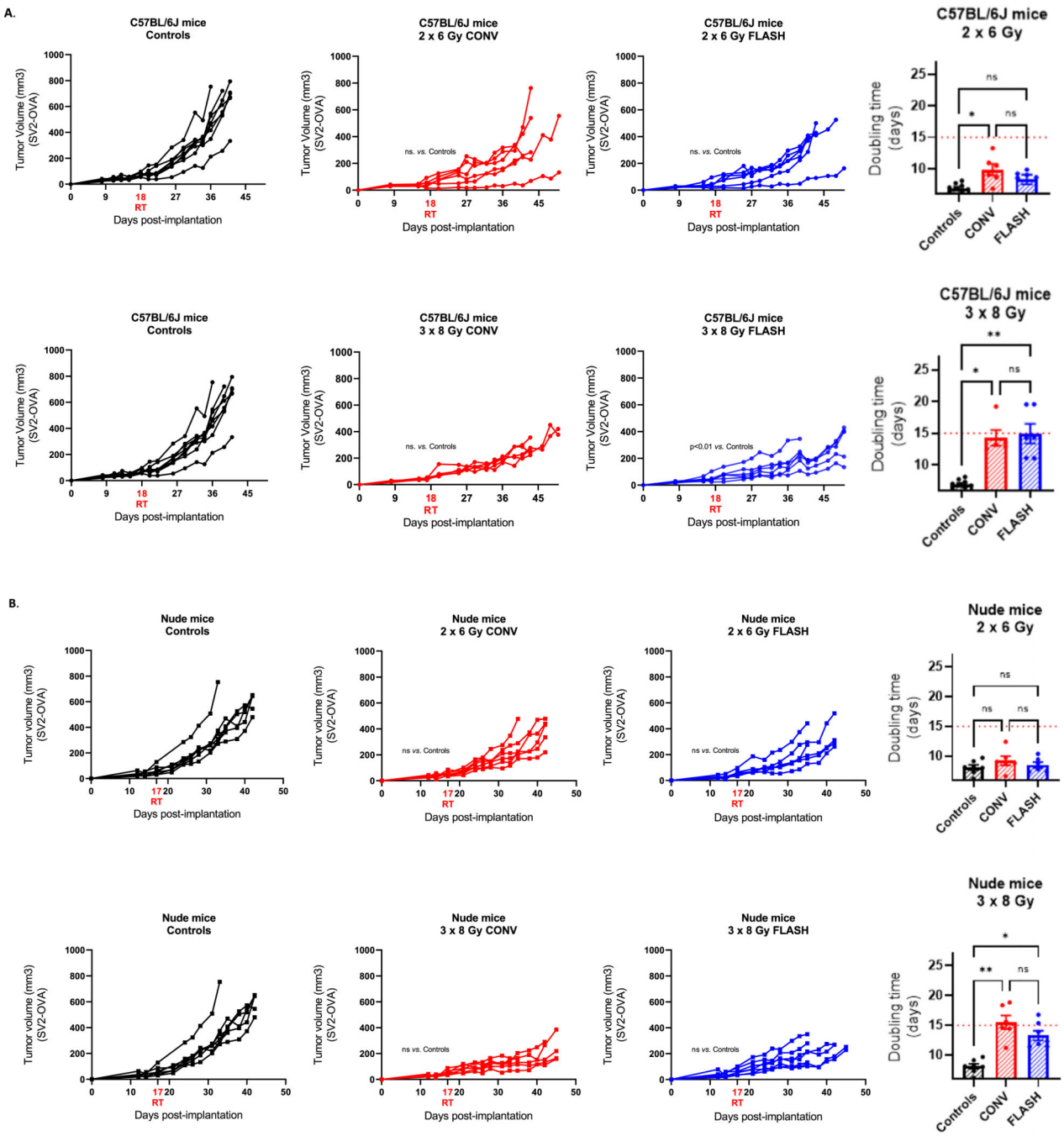

Fig. 2.

Fractionated regimens FLASH *versus* CONV have a similar antitumor effect that is not modified by the immune status of the host. SV2-OVA lung adenocarcinoma tumors were irradiated using hypofractionated regimens 2 × 6 and 3 × 8 Gy with FLASH or CONV after subcutaneous engraftment into immunocompetent C57BL/6J male mice (A) and immunodeficient Swiss nude male mice (B). Tumor growth was monitored by caliper measurement. Doubling time of tumors was determined using the model of exponential (Malthusian) growth from relative tumor growth curves on GraphPad Prism. Results are

given in mean + standard error of the means. Statistical analysis of growth curves was performed using Mann-Whitney test. Kruskal-Wallis with Dunn's multiple comparisons test was assessed for doubling time analysis. *$P < .05$, **$P < .01$, ***$P < .001$, ****$P < .0001$.

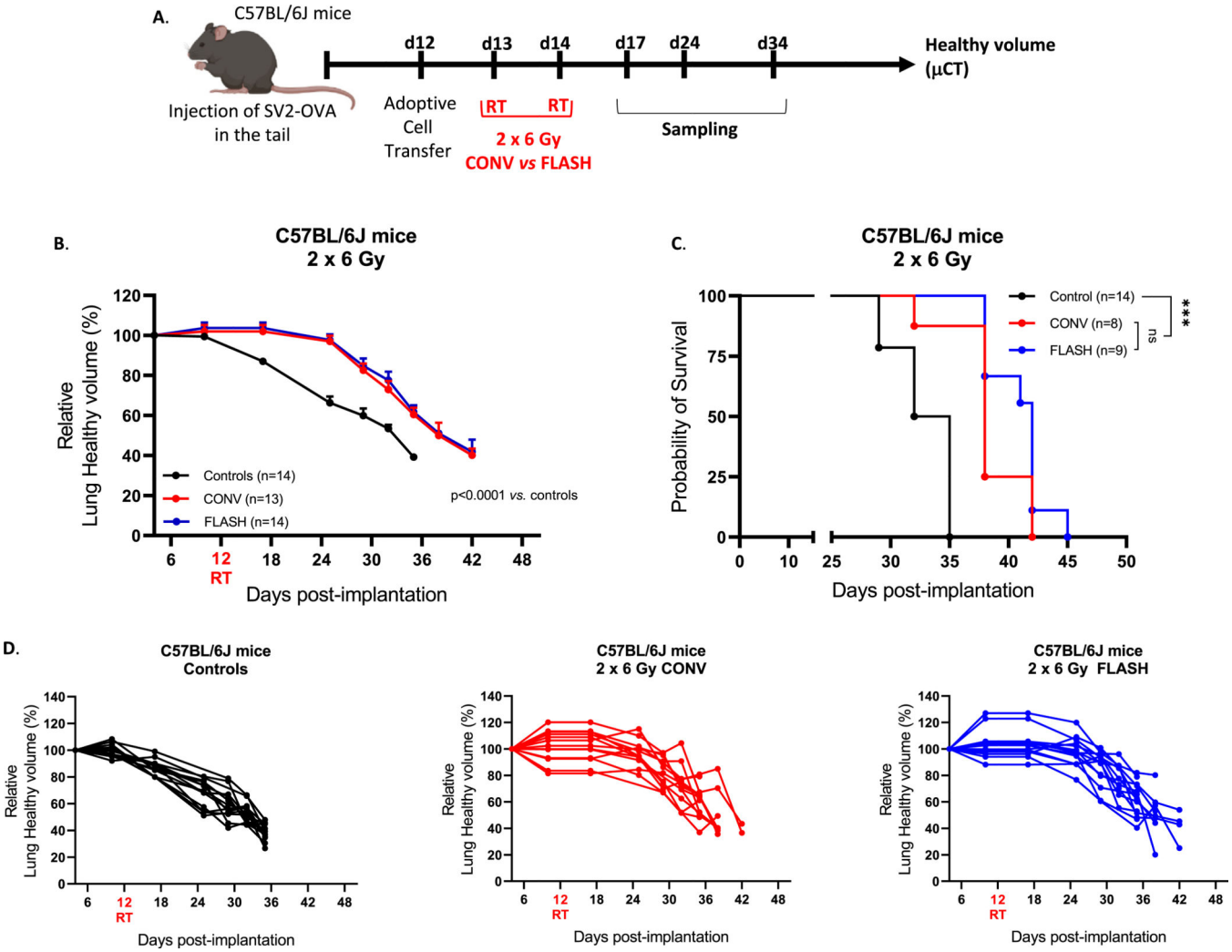

Fig. 3.

Fractionated regimens FLASH *versus* CONV have a similar antitumor effect when SV2-OVA lung ADK cells are implanted orthotopically. Orthotopic SV2-OVA lung adenocarcinoma was irradiated with 2 × 6 Gy FLASH and CONV after implantation in C57BL/6J male mice (A). Healthy lung volume (% of initial) was evaluated twice a week using micro-computed tomography imaging. Volumes were normalized to initial healthy volume determined before tumor implantation, and results were given in mean + standard error of the means (B) or individual values (D). Animal survival was followed over the time course of the experiment (C). Statistical analysis were performed using Mann-Whitney test for tumor growth. Log-rank (Mantel-Cox) test was used for survival curve analysis. $*P < .05$, $**P < .01$, $***P < .001$, $****P < .0001$. *Abbreviation:* CONV = conventional , ADK = adenocarcinoma

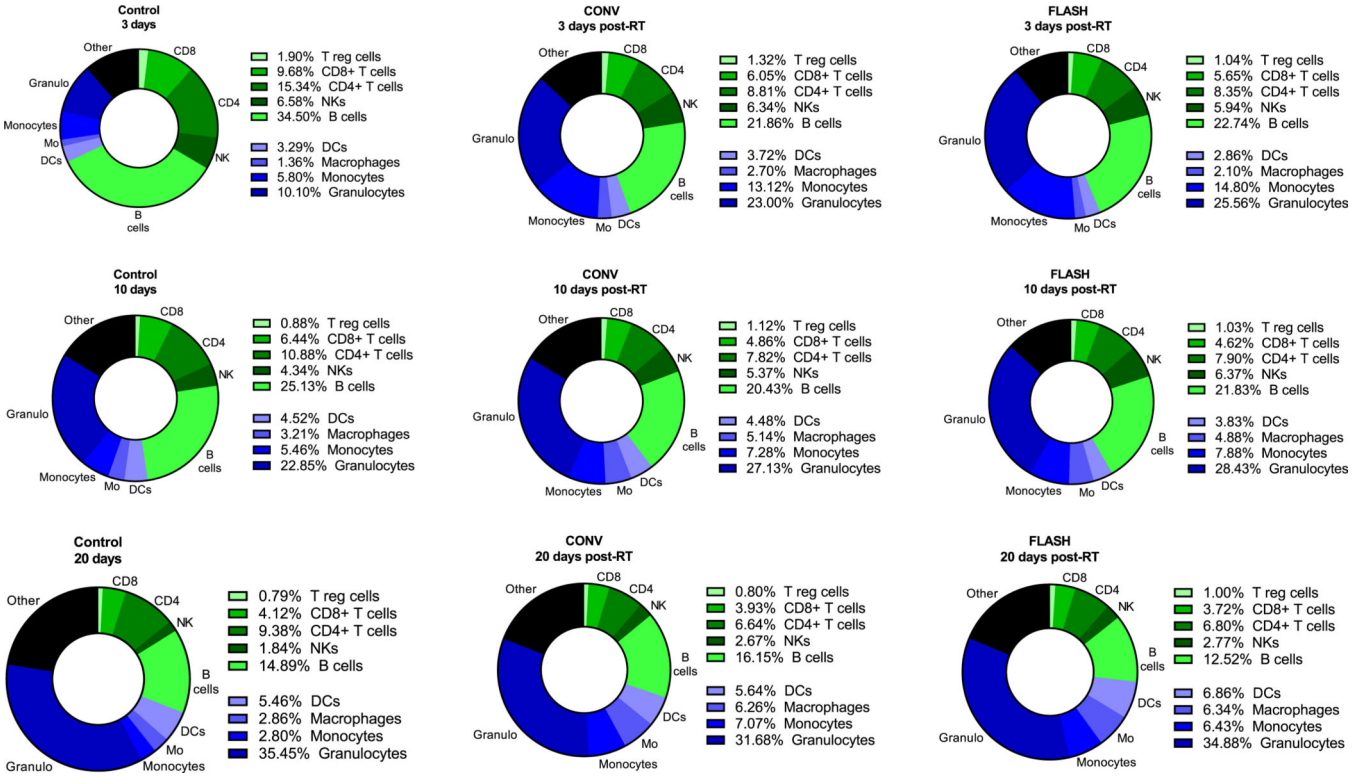

Fig. 4.

FLASH and CONV, 2 × 6 Gy, generate similar remodeling of the lung immune landscape. Orthotopic SV2-OVA lung adenocarcinoma was irradiated with 2 × 6 Gy FLASH or CONV after implantation in C57BL/6J male mice. Lungs were collected 3 days (day 17 post-implantation), 10 days (day 24 post-implantation), and 20 days (day 34 post-implantation) post radiation therapy, and the immune profile was evaluated by flow cytometry. Controls (n = 4–5), FLASH (n = 5–6), CONV (n = 5–6). Results are given in means and data are represented in part of the whole graph. *Abbreviation:* CONV = conventional.

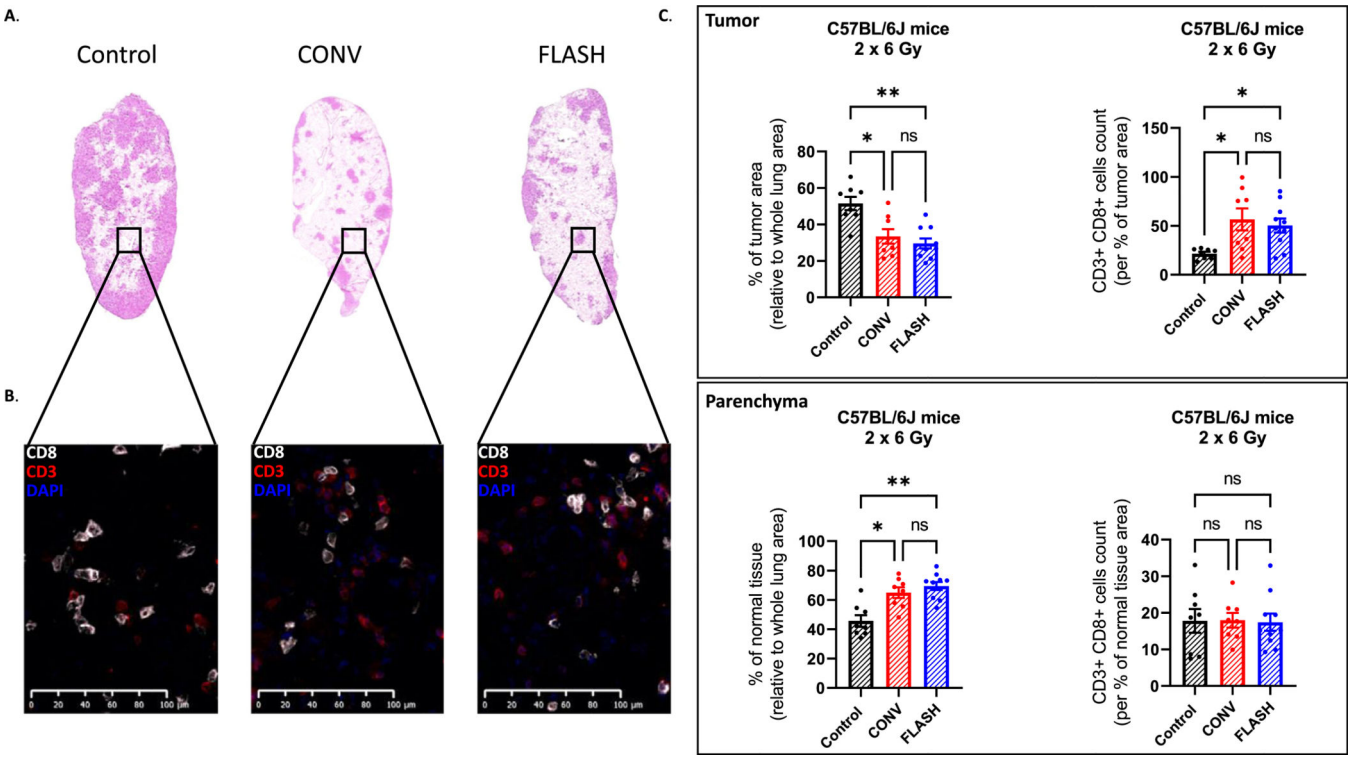

Fig. 5.

2 × 6 Gy FLASH and CONV generate similar CD8+ T cell infiltration in lungs bearing SV2-OVA lung adenocarcinoma. Thirty-four days post-implantation, lungs from C57BL/6J male mice were collected for immunohistochemistry and immunofluorescence staining. The percentage of tumor area, normal tissue (relative to whole lung area) (A, C), and CD3+ CD8+ cell count (B, C) were evaluated using QuPath software. Kruskal-Wallis with Dunn's multiple comparison was performed to compare the mean percentage of tumor area between groups. Results are depicted as mean + standard error of the means. *$P < .05$, **$P < .01$, ***$P < .001$, ****$P < .0001$.

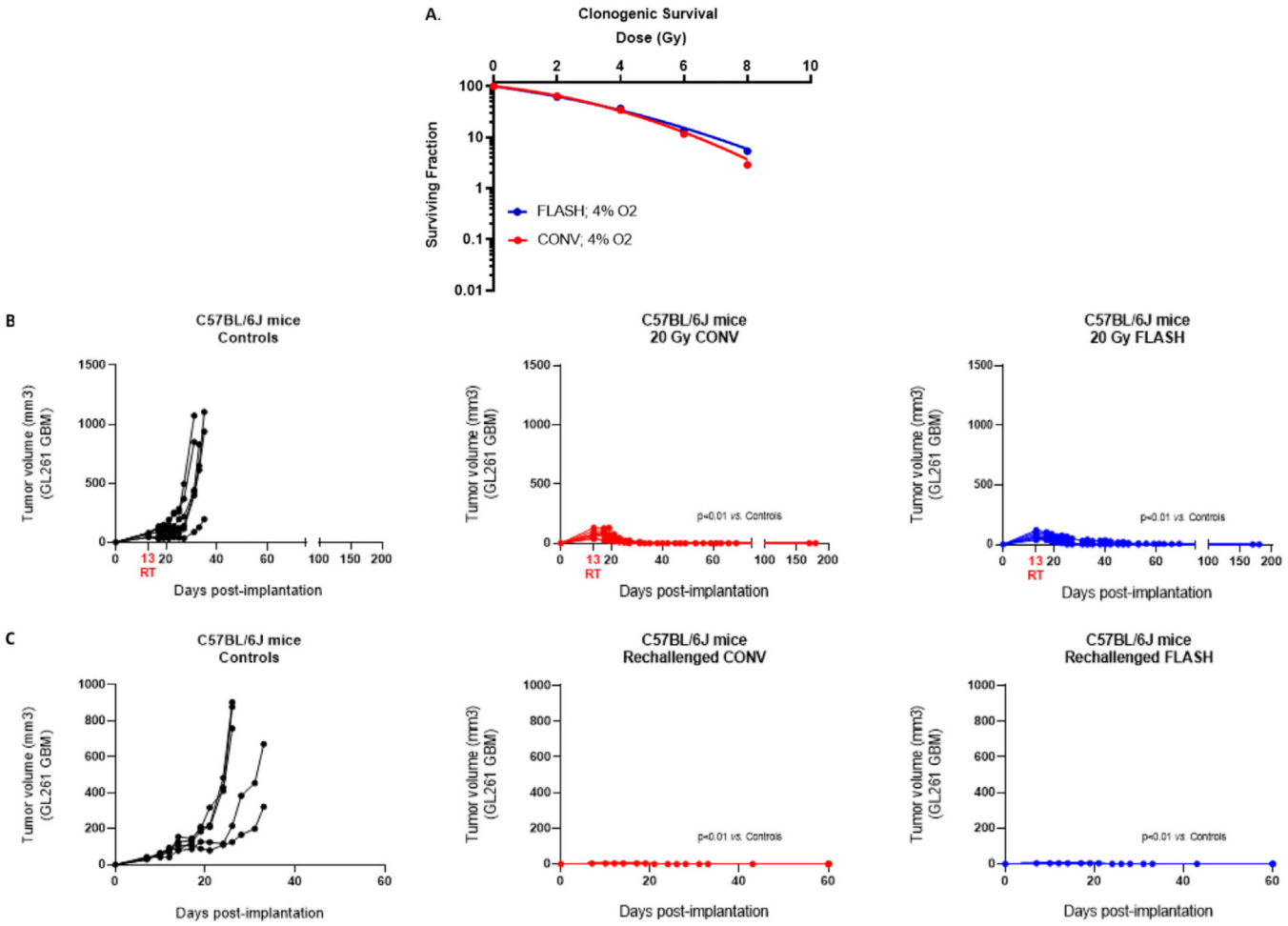

Fig. 6.

FLASH and CONV are equipotent in curing animals and generate a similar immunologic memory response against the GL261 cell line. Adherent GL261 tumor cells were irradiated from 2 to 8 Gy FLASH or CONV after incubation with 4% O_2 for 24 h (A). GL261 glioblastoma tumors were irradiated at 20 Gy with FLASH or CONV after subcutaneous engraftment into immunocompetent C57BL/6J female mice (B). Cured immunocompetent C57BL/6J female mice were rechallenged with 5×10^6 cells implanted in the opposite flank (C). Tumor growth delay was followed by caliper measurement 3 times per week. Results are given in individual values. Clonogenic survival curves were modeled using the linear quadratic model. Statistical analysis of tumor growth curves was performed using the Mann-Whitney test. $*P < .05$, $**P < .01$, $***P < .001$, $****P < .0001$. *Abbreviation:* CONV = conventional.